Accepted for publication of Mechanical Systems and Signal Processing, 2001

Vibration-Based Damage Detection Using Statistical Process Control

Michael L. Fugate[†], Hoon Sohn[‡], and Charles R. Farrar[‡]

Los Alamos National Laboratory
Los Alamos, NM 87545

Currently, vibration-based damage detection is an area of significant research activity. This paper attempts to extend the research in this field through the application of statistical analysis procedures to the vibration-based damage detection problem. The damage detection process is cast in the context of a statistical pattern recognition paradigm. In particular, this paper focuses on applying statistical process control methods referred to as "control charts" to vibration-based damage detection. First, an auto-regressive (AR) model is fit to the measured acceleration-time histories from an undamaged structure. Residual errors, which quantify the difference between the prediction from the AR model and the actual measured time history at each time interval, are used as the damage-sensitive features. Next, the X-bar and S control charts are employed to monitor the mean and variance of the selected features. Control limits for the control charts are constructed based on the features obtained from the initial intact structure. The residual errors computed from the previous AR model and subsequent new data are then monitored relative to the control limits. A statistically significant number of error terms outside the control limits indicate a system transit from a healthy state to a damage state. For demonstration, this statistical process control is applied to vibration test data acquired from a concrete bridge column as the column is progressively damaged.

1. INTRODUCTION

The potential economic and life-safety implications of early damage detection in aerospace, civil and mechanical engineering systems have motivated a significant amount of research in structural health monitoring. Many local damage detection methods have been developed and are routinely applied to a variety of structures [1]. Because of its potential for global system monitoring, damage detection as determined from changes in the vibration characteristics of a system has been a popular research topic for the last thirty years. Doebling et al. (1998) present a recent thorough review of these vibration-based damage identification methods [2]. While the references cited in this review propose many different methods for extracting damage-sensitive features from vibration response measurements, few of the cited references take a statistical approach to quantifying the observed changes in these features. However, because all vibration-based damage detection processes rely on experimental data with inherent uncertainties, statistical analysis procedures are necessary if one is to state in a quantifiable manner that changes in the vibration response of a structure are indicative of damage as opposed to operational and/or environmental variability. This paper will first pose the general problem of the vibration-based damage detection process in the context of a problem in statistical pattern recognition.

LAUR: 99-6231
[†] CIC Division, Computer Research & Applications Group, MS B265.
[‡] Engineering Sciences & Application Division, Engineering Analysis Group, ESA-EA, MS C926.

A damage detection study of a seismically retrofitted, reinforced concrete bridge pier is then described in the context of this paradigm. The paradigm was applied to the pier in its undamaged state and then after various levels of damaged had been introduced through cyclic loading. This discussion emphasizes the application of a statistical analysis procedure referred to as statistical process control (SPC) to the vibration-base damage detection problem. Although SPC is a well-established condition monitoring procedure for rotating machinery [13], the authors are not aware of applications of this technology to the vibration-based damage detection problem that includes civil infrastructure.

2. STATISTICAL PATTERN RECOGNITION PARADIGM

In the context of statistical pattern recognition the process of vibration-based damage detection can be broken down into four parts: (1) Operational Evaluation, (2) Data Acquisition and Cleansing, (3) Feature Extraction and Data Compression, and (4) Statistical Model Development.

Operational evaluation answers four questions in the implementation of a structural health monitoring system: (1) What are the life safety and/or economic justifications for monitoring the structure? (2) How is damage defined for the system being monitored? (3) What are the operational and environmental conditions under which the system of interest functions?, and (4) What are the limitations on acquiring data in the operational environment? Operational evaluation begins to set the limitations on what will be monitored and how to perform the monitoring as well as tailoring the monitoring to unique aspects of the system and unique features of the damage that is to be detected.

The *data acquisition* portion of the structural health monitoring process involves selecting the types of sensors to be used, the location where the sensors should be placed, the number of sensors to be used, and the data acquisition/storage/transmittal hardware. Other considerations that must be addressed include how often the data should be collected, how to normalize the data, and how to quantify the variability in the measurement process. *Data cleansing* is the process of selectively choosing data to accept for, or reject from, the feature selection process. Filtering is one of the most common methods for data cleansing.

The area of the structural damage detection process that receives the most attention in the technical literature is *feature extraction*. Feature extraction is the process of the identifying damage-sensitive properties derived from the measured vibration response that allows one to distinguish between the undamaged and damaged structures. Many different damage-sensitive features have been proposed including relatively simple ones such as the root-mean squared (RMS) and kurtosis of the response amplitudes [3], basic linear modal properties such as resonant frequencies and mode shapes, and quantities derived from them such as dynamic flexibility matrices [4]. For systems exhibiting nonlinear response, features such as an Aries Intensity Factor [5], features based on time-frequency analysis [6], and features derived from time series analysis [7] have shown promise for damage detection.

The diagnostic measurement needed to perform structural health monitoring typically produces a large amount of data. *Data compression* into small dimensional features is necessary if accurate estimates of the feature statistical distribution are to be obtained. The need for low dimensionality in the feature vectors is referred to as the "curse of dimensionality" and is discussed in detail in general texts on statistical pattern recognition [8].

The portion of the structural health monitoring process that has received the least attention in the technical literature is the development of statistical models to enhance the damage detection process. *Statistical model development* is concerned with the implementation of the algorithms that analyze the distributions of the extracted features in an effort to determine the damage state of the structure. The algorithms used in statistical model development usually fall into the three general categories of: (1) Group Classification, (2) Regression Analysis, and (3) Outlier Detection. The appropriate algorithm to use will depend on the ability to perform *supervised* or *unsupervised* learning. Here, supervised learning refers to the case were examples of data from damaged and undamaged structures are available. Unsupervised learning refers to the case were data is only available from the undamaged structure.

The statistical models are typically used to answer a series of questions regarding the presence and location of damage. When applied in a supervised learning mode and coupled with analytical models, the statistical procedures can be used to determine the type of damage, the extent of damage, and the remaining useful life of the structure. The statistical models are also used to minimize false indications of damage. False indication of damage falls into two categories: (1) *False-positive* damage indication (indication of damage when none is present), and (2) *False-negative* damage indication (no indication of damage when damage is present).

3. EXPERIMENTAL TEST

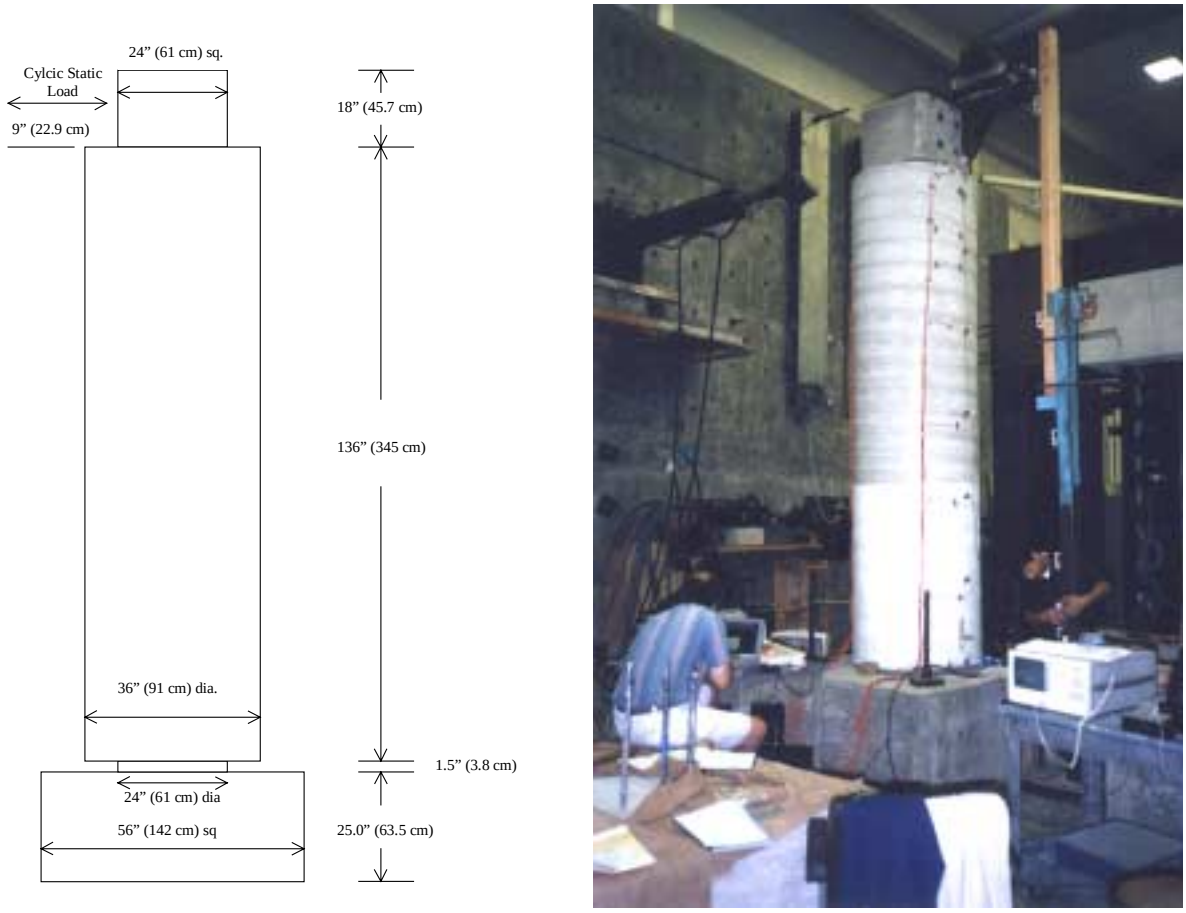

Figure 1: Column dimensions and photo of an actual test structure.

Faculty, students and staff at the University of California, Irvine (UCI) performed quasi-static, cyclic tests to failure on seismically retrofitted, reinforced-concrete bridge columns. Vibration tests were performed on the columns at intermittent stages during the static load cycle testing when various amounts of damage had been accumulated in the columns. The associated data obtained from one of the columns are used to investigate the applicability of statistical pattern recognition techniques to vibration-based damage detection problem.

The configuration of the test column and the dimensions are shown in Figure 1. The test structure was a 137.5 *in* (349 *cm*) long, 24 *in* (61 *cm*) diameter concrete bridge column that was subsequently retrofitted to a 36 *in* (91 *cm*) diameter column. The column was retrofitted by placing forms around the existing column and placing additional concrete within the form. A 24 in^2 concrete block, which had been cast integrally with the column, extends 18 *in* (46 *cm*) above the top of the circular portion of the column. This block was used to attach the hydraulic actuator to the column for quasi-static cyclic testing and to attach the electro-magnetic shaker used for the vibration tests. The column was bolted to the (25 *in*, 63.5 *cm* thick) testing floor in the UCI laboratory during both the static cyclic tests and vibration tests.

3.1 Test Procedure

A hydraulic actuator was used to apply lateral loads to the top of the column in a quasi-static, cyclic manner. The loads were first applied in a force-controlled manner to produce lateral deformations at the top of the column corresponding to $0.25\Delta y_T$, $0.5\Delta y_T$, $0.75\Delta y_T$ and Δy_T. Here, Δy_T is the lateral deformation at the top of the column corresponding to the theoretical first yield of the longitudinal reinforcement. The structure was cycled three times at each of these load levels. Next, a lateral deformation corresponding to the actual first yield Δy was estimated based on the observed response. Loads were then applied in a displacement-controlled manner, again in sets of three cycles, at displacements corresponding to $1.5\Delta y$, $2.0\Delta y$, $2.5\Delta y$, etc. until the ultimate capacity of the column was reached. The load-deformation response of the column during the quasi-static testing is shown in Figure 2.

Vibration tests were conducted on the column in its undamaged state, and after cycling loading at the subsequent displacement levels, Δy, $1.5\Delta y$, $2.5\Delta y$, $4.0\Delta y$, and $7.0\Delta y$. In this study, these vibration tests are referred to as damage level 0 thought 5, respectively. The excitation for the vibration tests was provided by an APS electro-magnetic shaker mounted off-axis at the top of the structure. The shaker rested on a steel plate attached to the top square block of the concrete column. Horizontal loading was transferred from the shaker to the structure through a friction connection between the shaker and the steel support plate. The shaker was controlled in an open-loop manner while attempting to generate 0 - 400 Hz uniform random signal. The RMS voltage level of this signal remained constant during all vibration tests. However, feedback from the column and the dynamics of the mounting plate produced an input signal that was not uniform over the specified frequency range.

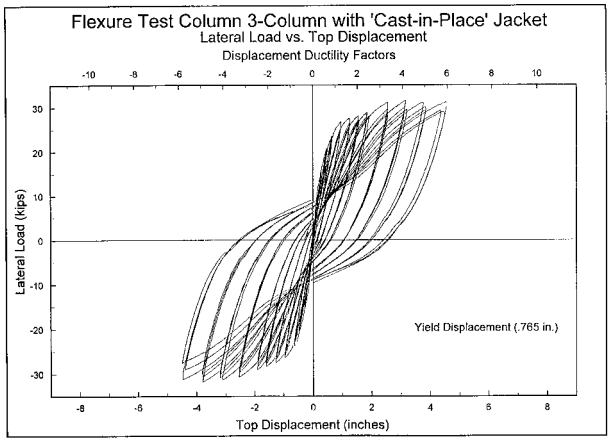

Figure 2: Load –displacement curves for the cast-in-place column

3.2 Operational Evaluation

Because the structure being tested was a laboratory specimen, operational evaluation was not conducted in a manner that would typically be applied to an *in situ* structure. However, the vibration tests were not the primary purpose of this investigation. Therefore, compromises had to be made regarding the manner in which the vibration tests were conducted. The primary compromise was associated with the mounting of the shaker where it would have been preferable to suspend the shaker from soft supports and apply the input at a point location using a stinger. These compromises are analogous to operational

constraints that may occur with *in situ* structures. Environmental variability was not considered an issue because the tests were conducted in a laboratory setting. The available dynamic measurement hardware and software placed the only constraints on the data acquisition process.

3.3 Data Acquisition and Cleansing

Forty accelerometers were mounted on the structure as shown in Figure 3. These locations were selected based on the initial desire to measure the global bending, axial and torsional modes of the column. Note that the accelerometer at locations 2, 39 and 40 had a nominal sensitivity of 10mV/g and were not sensitive enough for the measurements being made. As part of the data cleansing process, data from these channels were not used in subsequent portions of the damage detection process. Locations 33, 34, 35, 36, and 37 were accelerometers with a nominal sensitivity of 100mV/g. All other channels had accelerometers with a nominal sensitivity of 1V/g. An accelerometer on the sliding mass of the shaker provided a measure of the input force applied to the column. Analog signals from the accelerometers were sampled and digitized with a Hewlett-Packard (HP) 3566A dynamic data acquisition system. Data acquisition parameters were specified such that unwindowed 8-second time-histories were discretized with 8192 points. Anti-aliasing filters were applied to further cleanse the data. Analog and digital anti-aliasing filters with cut off frequencies of 12.8 kHz and 512 Hz, respectively, were used. Data decimation was also used to cleanse the data. Although the data are sampled at 25.6 kHz, the decimation process yields an effective sampling rate of 1.024 kHz. Finally, an AC coupling filter that attenuates signal below 2 Hz was applied to remove DC offsets from the signal.

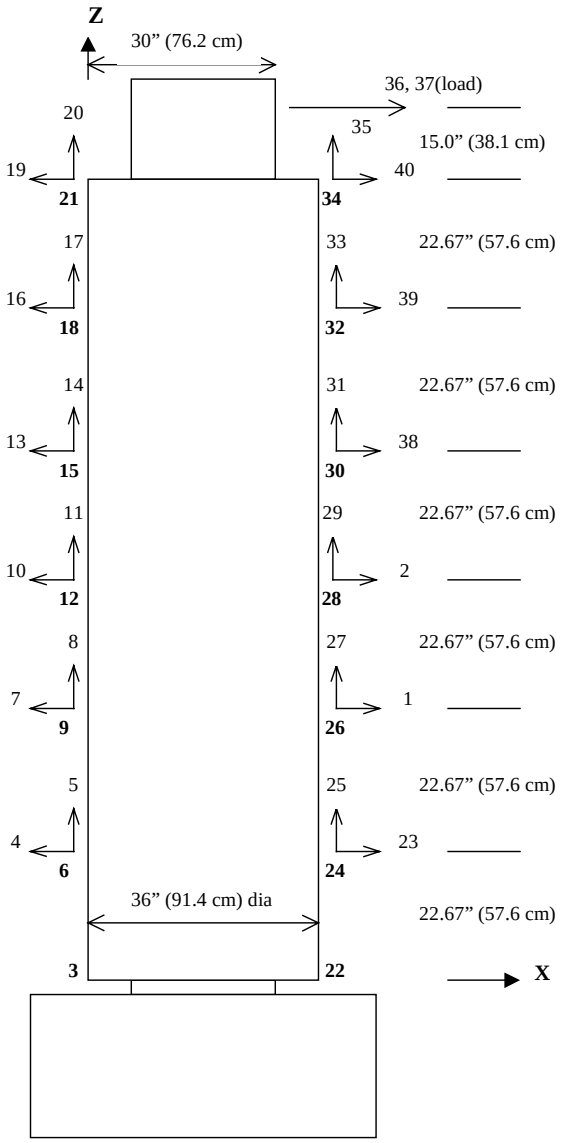

Figure 3: Placement of accelerometers used during vibration testing

4. STATISTICAL PROCESS CONTROL

In this section statistical process control (SPC) and its application to vibration-based damage detection is discussed. Damage sensitive data features derived from acceleration measurements, $x(t)$, taken when the structure is in good condition will have some distribution with mean μ and variance σ^2. If the structure is damaged the mean, the variance of these features, or both might change. Statistical process control provides a framework for monitoring future extracted data features and for identifying new data that are inconsistent with past data. In particular, quality control charts are proposed to monitor the mean, the variance, or some other function of these damage sensitive features.

4.1 Feature Extraction Based on Auto-Regressive Modeling

If the acceleration measurements are autocorrelated, constructing a control chart that ignores the correlation can lead to charts that give many false alarms and charts that fail to signal when the process being monitored has changed significantly; see [9] and the references therein. Because the acceleration measurements will be autocorrelated, we suggest constructing an *X*-chart or an *X*-bar chart using the residuals obtained from fitting an autoregressive (AR) model to the observed data. If the fitted AR model is approximately correct, the residuals from the fit should be (nearly) uncorrelated with no systematic pattern.

An AR model with *p* autoregressive terms, AR(p), can be written

$$x(t) = a + \sum_{j=1}^{p} \phi_j \; x(t-j) \; + z(t) \; . \qquad (1)$$

where $x(t)$'s are acceleration measurements observed at time t and $z(t)$ is an unobservable random error with mean 0 and constant variance. The mean of the $x(t)$ is μ for all t and $a \equiv \left(1 - \sum \phi_j\right)\mu$. The ϕ_j's and μ are unknown parameters that must be estimated. In this study the AR coefficients are estimated by the Yule-Walker method [10].

To fit an AR model to observed data, the order of the model, *p*, needs to be chosen and the parameters need to be estimated. There are a variety of techniques for choosing the model order, such as Akaike's Information Criterion (AIC) and for estimating the parameters. These techniques can be found in most textbooks on time series, e.g. [10].

If $\hat{x}(t)$ denotes the estimated acceleration measurement from the fitted AR model, then the residual at time t is $e(t) = x(t) - \hat{x}(t)$. An *X*-bar chart can be constructed with the residuals as data. If the fitted model is approximately correct, the residuals should be nearly uncorrelated. Note that for a fitted AR(p) model residuals cannot be computed for $t \leq$ p. From a pattern recognition perspective, the residuals can be thought of as features derived from the measured time histories.

When new data become available, the current acceleration measurement is predicted using these data and the AR model whose estimated parameters were based on the initial, or undamaged data. A new vector of residual errors is then determined. These new residual errors or the average residual error from rational subgroups are then charted. If there is damage, the AR model should not fit the new acceleration measurements very well and a statistically significant number of residuals or average residuals should chart beyond the control limits.

As mentioned previously, it is possible for environmental factors such as wind, rain, and temperature, to affect the acceleration measurements on *in situ* structures. Observed environmental and operational factors can be incorporated directly into the AR model by simply adding a parameter for each factor of interest along with observed values of the factor. Alternatively, the observed acceleration measurements can be regressed on the observed environmental and operational factors and the residuals computed. An AR model could then be fit to the residuals.

4.2 Construction of X-bar Control Chart

In this section we discuss the construction of an *X*-bar control chart using the time history acceleration measurements taken before the column was damaged, denoted as damage level 0. An AR(5) model is fitted to this data. The choice of an AR(5) model is discussed in section 5.1.

To detect a change in the mean of the acceleration measurements, an intuitively appealing idea is to form rational subgroups of size *n*, compute the sample mean, μ, within each subgroup and chart the sample means. The centerline for this control chart will be μ but the standard deviation of the charted values would be $\sigma/\sqrt{n}$. Therefore, the control limits would be placed at $\mu \pm k\sigma/\sqrt{n}$. This type of control chart is referred to as an *X*-bar chart, see [9]. In this study an X-bar control chart is constructed based on the residuals from this fitted model using subgroups of size 4. Note that the subgroup size *n* is chosen so that observations within each group are, in some sense, more similar than observations between groups. If *n* is chosen too large a drift that may be present in the mean can possibly be obscured, or averaged-out. An additional motivation for charting sample means, as opposed to individual observations, is that the distribution of the sample means can, by an application of a central limit theorem, be approximated by a normal distribution.

As mentioned previously, there are 8192 acceleration measurements. Residuals can be computed for acceleration measurements 6 through 8192. For convenience the last 3 residuals are discarded which leaves 8184 residuals. Subgroups of size 4 are constructed by placing the residuals for observations 6 through 9 in the first group, 10 through 13 in the second group and so on. This process produces 2046 subgroups of residuals each of size 4. The charted values are the sample means from each subgroup, denoted by $\bar{x}_1, \ldots, \bar{x}_{2046}$.

Prior to computing subgroup means and variances, the 8184 residuals, from damage level 0, are normalized by subtracting their sample mean and dividing by their sample standard deviation, $\hat{\mu}_0$ and s_0, respectively. The residuals from damage levels 1 through 5 are also adjusted by subtracting $\hat{\mu}_0$ and dividing by s_0 from the damage level 0 data.

The centerline of the chart is the sample mean of the charted values. This centerline is the sample mean of the residuals from observations 6 through 8189, and, after the normalization just described, is 0. The sample variance of each subgroup is determined and these variances are then averaged to give a pooled estimate of variance. A simple average is appropriate because each subgroup is size 4. The square root of the pooled variance, s_p, is used as an estimate of the population standard deviation. Control limits are drawn at $0 \pm z_{\alpha/2}\, s_p/\sqrt{n}$ where $n = 4$ and z_α represents the α quantile of the standard normal distribution. For the examples in this paper, α was chosen to be 0.01.

4.3 Construction of S Control Chart

To monitor variability within each subgroup, an S control chart can be used. For each subgroup the sample standard deviation of the (normalized) residuals is computed. These sample standard deviations from each subgroup, s_j for $j = 1, \ldots, 2046,$ become the charted values. The upper and lower control limits (UCL and LCL) are

$$\text{UCL} = \bar{S}\sqrt{\frac{\chi_{1-\alpha/2,n-1}}{n-1}} \quad \text{and} \quad \text{LCL} = \bar{S}\sqrt{\frac{\chi_{\alpha/2,n-1}}{n-1}}\,. \tag{2}$$

where $\chi^2_{p,n}$ denotes the *p*th quantile of a Chi-square random variable with *n* degrees of freedom and $\bar{S}$ is the average of s_j for $j = 1,\ldots,2046$. Again, in the examples α was chosen to be 0.01.

5. EXPERIMENTAL RESULTS

The applicability of the X-bar and S control charts to damage diagnosis problems is demonstrated using the vibration test data obtained from the test column shown in Figure 1. Results are presented for data obtained from measurement point one, shown in Figure 3. Although the results obtained from the other accelerometers are not presented here, similar conclusions are observed for most of the other measurement points. Sohn et al. (1999) applied SPC to a Principal Component Analysis (PCA) of the time series from all measurement points [10].

5.1 Order Selection of the AR Model

Before discussing control charts applied to the data from damage levels 1-5, the order of the AR model is discussed. Figure 4 (a) shows the autocorrelation between acceleration measurements from damage level 0. For lag 1 the correlation is greater than 0.80. The most striking feature of the plot is that the autocorrelations are *not* dying out particularly fast. In fact, the autocorrelations are statistically significant for lags greater than 100. To remove the correlation an AR(5) model was fitted to the damage level 0 data. An autocorrelation plot of the residuals from this model is shown in Figure 4 (b). While the autocorrelation plot of the residuals from the AR(5) model is far from ideal, the AR(5) model has reduce the correlation for all lags to less than 0.20 and most of the lags have correlation less than 0.10. For residuals that are 1, 2, and 3 time units apart, the correlation is nearly 0.

Recall that subgroups are constructed by placing 4 consecutive residuals together. This means that the largest lag within a group is 3. As such, the residuals within each subgroup are essentially uncorrelated. Because the residuals within each subgroup are nearly uncorrelated, the sample variance within each subgroup is for practical purposes an unbiased estimate of the population variance.

A number of higher order AR models were fitted to the data without significantly changing the appearance of the autocorrelation plot in Figure 4 (b). For example, with an AR(19) model the autocorrelations through lag 30 were eliminated but the oscillatory pattern in the plot remained and there was still statistically significant correlation beyond lag 30. The performance of the control chart using the AR(19) model was not significantly better than that of the AR(5). Also, several autoregressive moving average models were fit but the results were essentially the same as with fitting higher order AR models. The results indicate that there is no compelling reason to fit a model more complicated than the AR(5).

For each damage level, 0 through 5, there are 8192 acceleration measurements. The AR(5) model determined from damage level 0 data is used to predict the acceleration measurements for damage levels 1 through 5 and the residuals are determined. The residuals are grouped into subgroups of size 4, exactly as was done for the undamaged data; this gives 2046 subgroups each of size 4.

For the *X*-bar chart the charted values are the sample means from each subgroup. In the *S*-chart the charted values are the sample standard deviations from each subgroup.

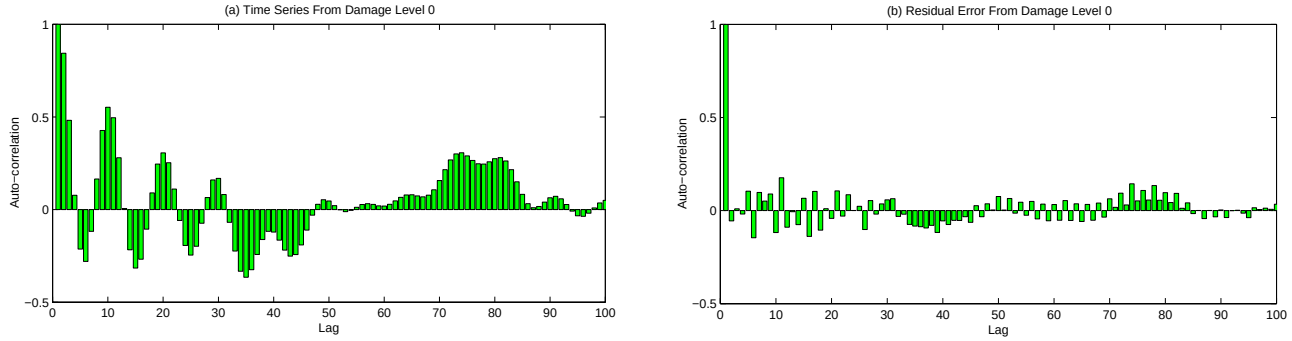

Figure 4: Removal of correlation using AR(5) model.

5.2 X-bar Control Chart Analysis

Figure 5 shows the control charts for all damage levels. In these charts, CL, UCL, and LCL denote the centerline, upper and lower control limits, respectively. Outliers correspond to subgroup sample means outside the control limits and are marked by a "+".

Because $\alpha = 0.01$, approximately 20 charted values (= 1 % of total 2046 samples) are expected to be outside the control limits even when the system is in control. Therefore, the 13 outliers in Figure 5 (a) are not unusual and do not indicate any system anomaly for damage level 0. However, a statistically significant number of outliers are observed for damage levels 1 though 5.

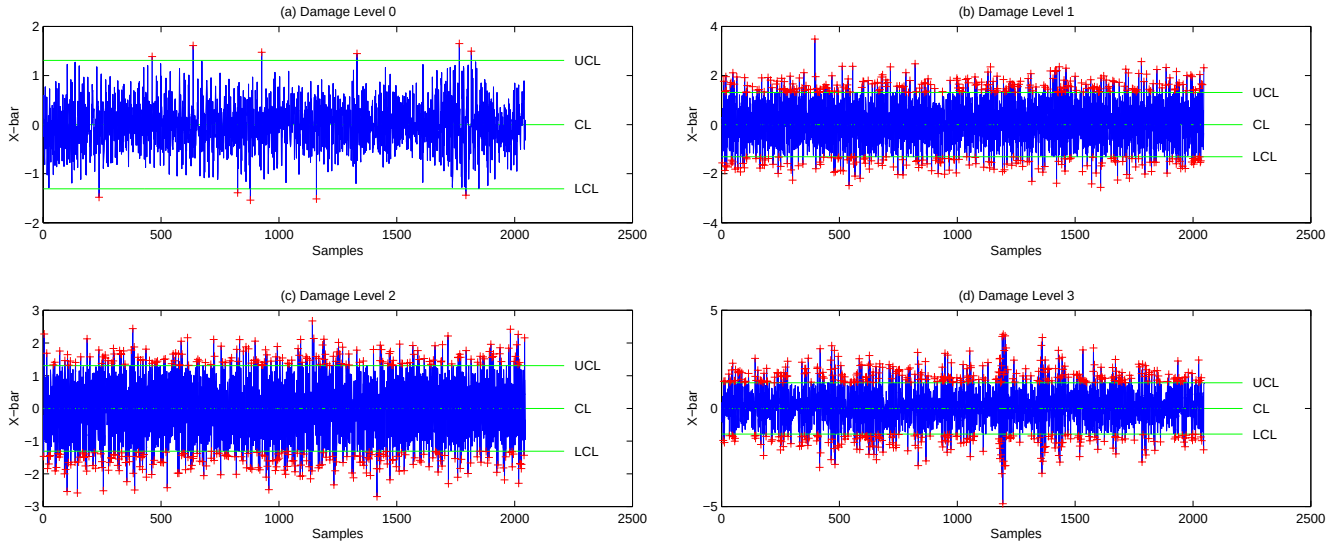

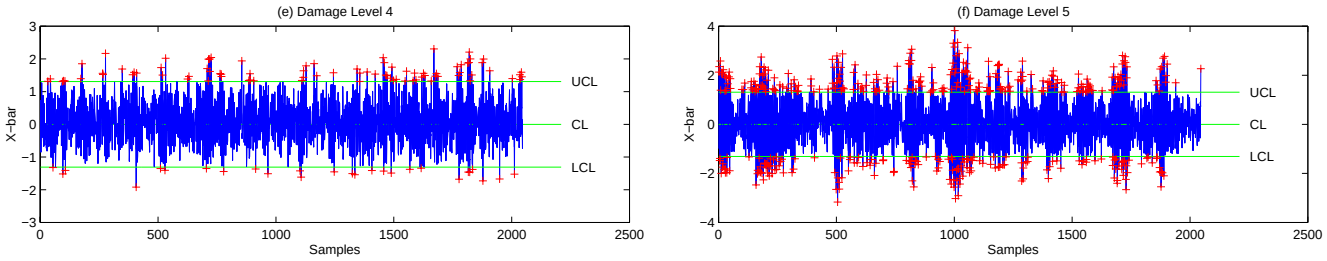

Figure 5: X-bar control chart of the residual errors

5.3 S Control Chart Analysis

Figure 6 shows the S control chart for damage levels 0 through 5. As with the X-bar charts, when there is no damage at most 1% of the charted values should fall outside the control limits. For damage level 0 there are 16 outliers. Damage levels 1 through 5 all show a significant number of outliers. In particular, most of the outliers are above the upper control limit, implying that the variance has increased.

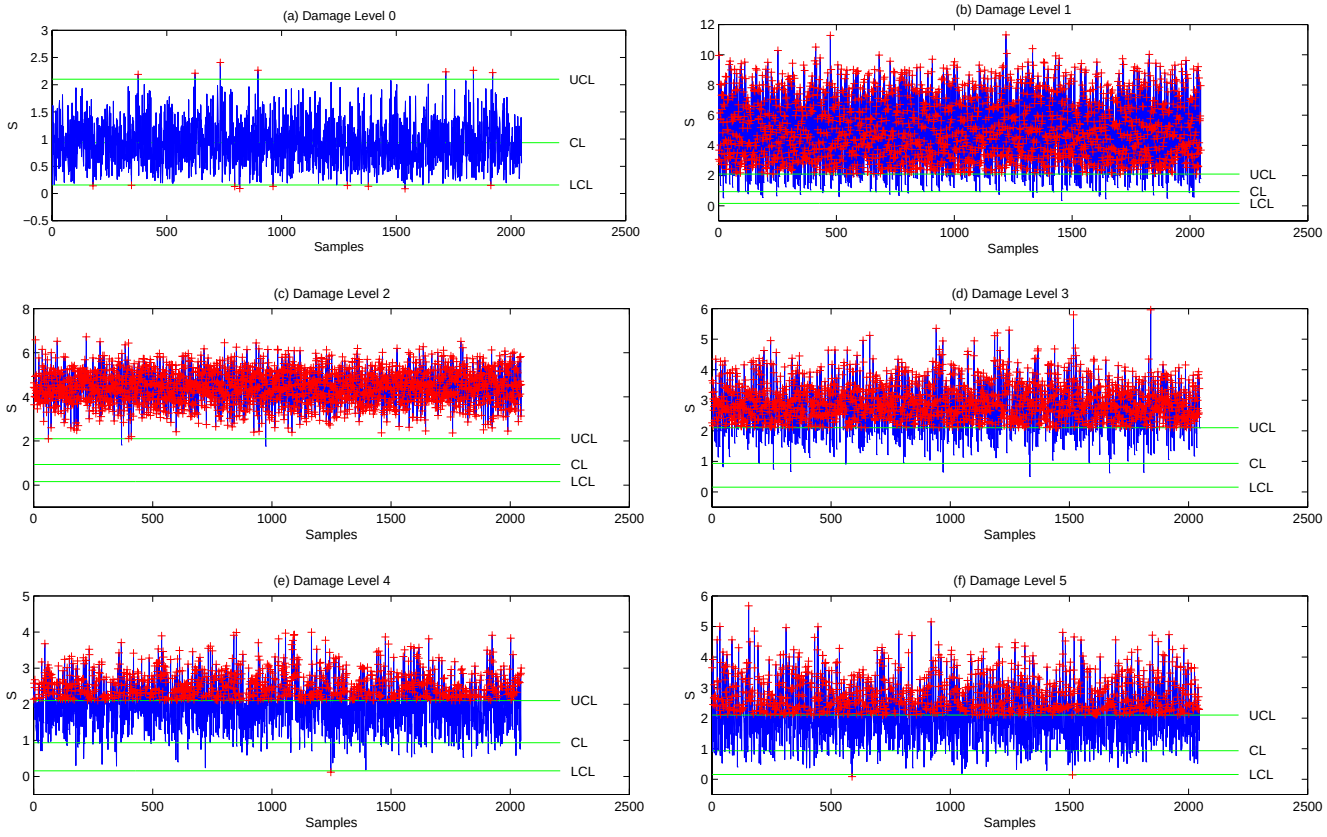

Figure 6: S control chart of the residual errors

5.4 False-Positive Testing

While it is desirable to have features sensitive to damage, the monitoring system also needs to be robust against a false-positive indication of damage; false-positive indication of damage means that the monitoring system indicates damage although no damage is present. To investigate the robustness of the proposed control charts, two separate tests were designed.

In the first test, damage level 0 data is divided into two parts and control limits are constructed from the first half of the time series. The second half of the data is used to test for false alarms.

The original time series is 8-seconds long with 8192 time points and each half of the series is 4-seconds long with 4096 points. An AR(5) model is fitted to the first half of the data to estimate the AR coefficients; the second half of the series is then predicted using this model. Residuals are computed for both sets of data. In all there are 1022 subgroups of size 4. Note that the last three residual terms are simple ignored, i.e. $1022 \times 4 + 3 = 4096 - 5$.

Figure 7 (a) and Figure 8 (a) show the X-bar and S control charts for the first half of the data. Figure 7 (b) and Figure 8 (b) show the X-bar and S control charts applied to the second half of the time series. Again, we expect to see at most 1% of the charted values outside the control limits. For both the X-bar and S control chart, less than 1% of the charted values are beyond the limits.

For the second test, an independent 2-second time series, measured from a separate vibration test of the undamaged column was available. Using the model and control charts developed for the damage level 0 data, an X-bar and S control chart were constructed for this independent data. The control charts are in Figure 7 (c) and Figure 8 (c). Fewer than 5 outliers (1% of 500 subgroups) are observed in each chart.

These two false-positive studies provide evidence that both the X-bar and S control charts are robust against false-positive indication of damage.

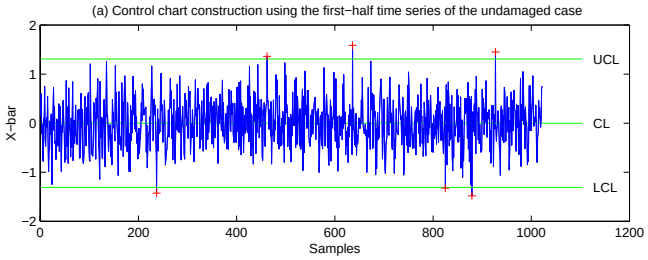

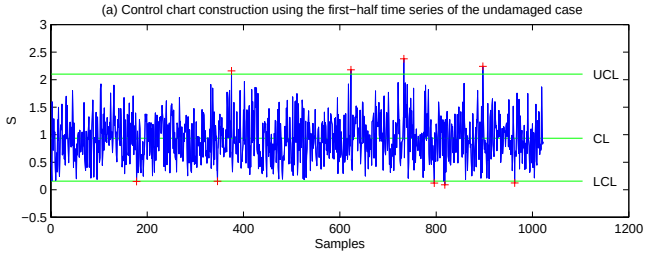

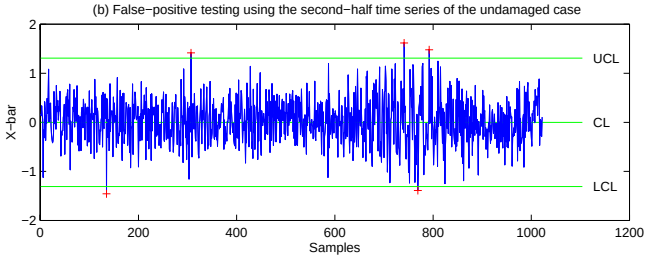

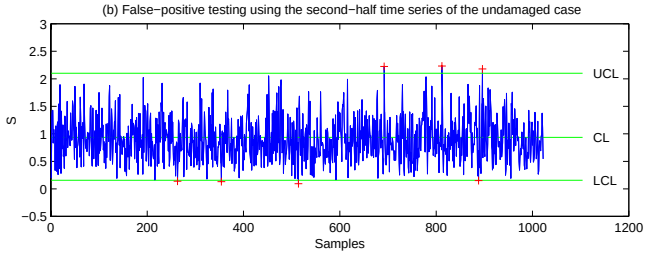

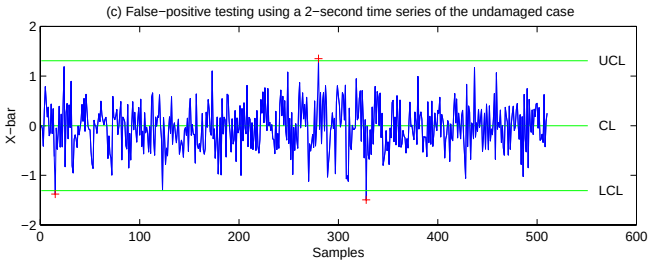

Figure 7: False-positive testing using X-bar control chart

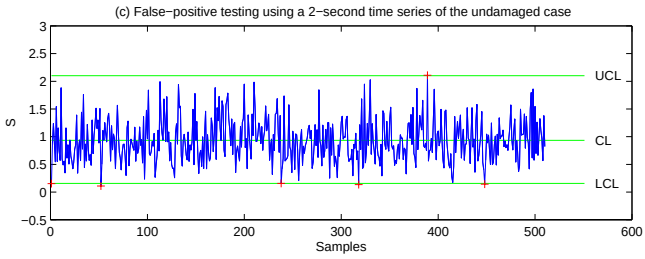

Figure 8: False-positive testing using S control chart

6. SUMMARY AND CONCLUSIONS

This paper has presented vibration-based damage detection problems in the context of statistical pattern recognition. The point of view taken in the paper is that in most cases vibration-based damage detection must be performed in an unsupervised learning mode because the training data available is only from an undamaged structure. If training data were available from both a damaged and an undamaged structure, supervised learning methods for statistical pattern recognition would be applicable.

Statistical process control using control charts was applied in an unsupervised learning mode to the vibration test data obtained from the bridge column in its undamaged state and after various levels of damage have been introduced. X-bar and S control charts, developed from time histories measured on the undamaged structure, were used to monitor the mean and variance of residuals, obtained from fitting an AR(5) model to the observed acceleration measurements. The assumption here is that the residuals are a damage sensitive feature derived from the measured data. The basis for this assumption is that there will be a significant increase in the residual errors when an AR model developed from the undamaged linear system response is used to predict the response from a damaged system exhibiting nonlinear response. In this manner, the statistical process control procedures are being used only to identify the existence of the damage. For long term monitoring a statistical process control framework is very attractive. Once a feature of interest has been chosen or constructed, the distribution of this feature can be estimated and then, automatically, future observations can be monitored to see if the feature distribution has changed significantly. If a significant change has occurred, a warning signal can be sent to the appropriate people.

For all investigated damage levels, the control charts successfully indicated some system anomaly. The strongest indication of damage, as identified by the number of points outside the control limits, is associated with damage case one. Fewer outliers, compared to the other damage levels, were detected for damage levels 4 and 5. Although not rigorously verified, it is speculated that this trend in damage indication is related to yielding of the rebar. The first damage level corresponds to incipient yielding of the rebar. Because of strain compatibility, this incipient yielding is accompanied by cracking of the concrete. The shaker, which was driven with the same input voltage level during each test, is most likely to cause nonlinear response associated with the cracks opening and closing at this first damage level. At the higher damage levels, the rebar has yield significantly. When load is removed from the column, this yielding tended to hold the cracks in an open configuration during the subsequent dynamic

tests. The excitation provided by the shaker could not excite the nonlinearities associated with cracks opening and closing to the same degree when the rebar had yielded significantly.

The robustness of the proposed control charts against a false-positive warning of damage was also demonstrated using two separate tests. These tests gave no indication that the control charts would produce a false-positive indication of damage. False-positive indications of damage can arise when the data features are correlated. Correlated data lead to the underestimation of control limits. The use of residual errors as damage sensitive features removed correlation in the data being monitored by the control charts.

In general, the observation of a large number of outliers does not necessarily indicate that a structure is damaged but only that the system has varied to cause statistically significant changes in its vibration signature. This variability could be caused by a variety of environmental and operational conditions that the system of interest is subject to. Operational and environmental conditions such as wind, humidity, intensity and frequency of traffic loading should be taken into account, and to the extent possible monitored, for applications to full-scale civil engineering infrastructure. Statistical process control provides a framework to account for these additional sources of variability and is a current focus of research for the authors.

Attention in this paper was focused on the time-history measurements from one sensor to illustrate the use of control charts. Although not reported in detail, various individual sensors were analyzed using the same procedures described in this paper. Results from these various sensors were similar to those previously summarized herein. With 40 sensors located on the test column several different approaches are possible for simultaneously analyzing data from all the sensors for indications of a damaged system. For example, a principal component analysis could be done to reduce the 40 dimensional time-history vector to a one, two, or three dimensional feature vector. A control chart, or multivariate control chart, could then be constructed based on this lower dimensional feature vector. This approach is currently under investigation by the authors.

Finally, the success of structural health monitoring will depend crucially on the selected damage-sensitive features. If the distribution of the chosen feature**s** does not change in a meaningful way when the structure is damaged**,** then it is doubtful if monitoring these features will yield useful information regarding the structural health of the system no matter what statistical pattern recognition algorithm is applied.

7. ACKNOWLEDGEMENT

Portion of the funding for this work has come from a cooperative research and development agreement with Kinemetrics Corporation, Pasadena California. The civilian application of this CRADA is aimed at developing structural health monitoring systems for civil engineering infrastructure. A portion of the funding for this research was provided by the Department of Energy's Enhanced Surveillance Program. Vibration tests on the column were conducted jointly with Prof. Gerry Pardoen at the University of California, Irvine using Los Alamos National Laboratory's University of California Interaction Funds. CALTRANS provided the primary funds for construction and cyclic testing of the columns

8. REFERENCES

1. Doherty, J. E., “Nondestructive Evaluation,” Chapter 12 in *Handbook on Experimental Mechanics*, A. S. Kobayashi Edt., Society for Experimental Mechanics, Inc., 1987
2. Doebling, S. W., C. R. Farrar, M. B. Prime and D. W. Shevitz, (1998) "A Review of Damage Identification Methods that Examine Changes in Dynamic Properties," *Shock and Vibration Digest* **30** (2).
3. H. R. Martin, (1989) “Statistical Moment Analysis as a Means of Surface Damage Detection”, *Proceedings of the 7th International Modal Analysis Conference*, pp. 1016-1021, Las Vegas, NV.
4. Farrar, C. R. and D. V. Jauregui (1998) "A Comparative Study of Damage Identification Algorithms Applied to a Bridge: Part I, Experimental" *J. of Smart Materials and Structure*, **7**.
5. Straser, E. G. (1998) “A Modular, Wireless Damage Monitoring System For Structures,” Ph. D. Dissertation, Dept. of Civil Eng., Stanford Univ., Palo Alto, CA.
6. Prime, M. B. and D. W. Shevitz (1996) “Linear and Nonlinear Methods for Detecting Cracks in Beams,” *Proceedings of the 14th International Modal Analysis Conference*, Dearborn, MI.
7. Hunter, N. F. (1999) “Bilinear System Characterization from Nonlinear Time Series Analysis,” *Proceedings of the 17 th International Modal Analysis Conference*, Orlando, FL.
8. Bishop, C. M., *Neural Networks for Pattern Recognition*, Oxford University Press, Oxford, UK, 1995.
9. Montgomery, D. C., *Introduction to Statistical Quality Control*, John Wiley & Sons, Inc., New York, 1996.
10. Brockwell, P. J. and Davis, R. A., *Time Series: Theory and Methods*, Springer, New York, 1991.
11. Sohn, H., Czarnecki, J. J., and Farrar, C. R., “Structural Health Monitoring using Statistical Process Control and Projection Techniques,” will be submitted to Journal of Structural Engineering, ASCE, 1999.
12. Box, G. E., Jenkins, G. M., and Reinsel, G. C., *Time Series Analysis: Forecasting and Control*, Prentice-Hall, Inc., 1994.
13. Wowk, V., *Machinery Vibration Measurement and Analysis*, McGraw-Hill, Inc. New York, 1991.